

MULTI-STRANGE BARYON PRODUCTION  
IN Pb–Pb COLLISIONS AT  $\sqrt{s_{NN}} = 2.76$  TeV  
WITH THE ALICE EXPERIMENT AT THE LHC\*

MARIA NICASSIO

for the ALICE Collaboration

Dipartimento Interateneo di Fisica ‘M. Merlin’ and Sezione INFN  
Via Orabona 4, 70126 Bari, Italy

(Received January 9, 2012)

Preliminary results by the ALICE Collaboration at the CERN Large Hadron Collider are presented for the multi-strange baryons in Pb–Pb collisions at  $\sqrt{s_{NN}} = 2.76$  TeV. Mid-rapidity transverse momentum spectra of the charged  $\Xi$  and  $\Omega$  baryons are shown in 0–90% centrality as well as in four centrality classes. The enhancements with respect to  $pp$  collisions at the same centre-of-mass energy have also been studied as a function of the mean number of participating nucleons and compared to existing measurements at SPS and RHIC.

DOI:10.5506/APhysPolBSupp.5.237

PACS numbers: 25.75.–q, 25.75.Dw, 25.75.Nq, 12.38.Mh

## 1. Introduction

The study of strange and multi-strange particle production in relativistic heavy-ion interactions is an important tool to investigate the properties of the strongly interacting system created in the collision, as there is no net strangeness content in the colliding nuclei. In particular, baryons with more than one unit of strangeness are very useful probes of the early partonic stages of the collision due to their small hadronic cross-section.

The enhancement of strangeness production in relativistic heavy-ion collisions relative to proton-induced reactions was one of the predicted signatures of the quark-gluon plasma formation [1]. This enhancement was first observed at SPS, confirmed afterwards by data at RHIC, and was notably more pronounced for multi-strange particles than for single-strange particles [2]. The original assumptions, on which the explanation of strangeness

---

\* Presented at the Conference “Strangeness in Quark Matter 2011”, Kraków, Poland, September 18–24, 2011.

enhancement was based, have gone through further theoretical developments and alternative mechanisms for strangeness production have been suggested [3]. The ALICE data can provide additional constraints to the interpretation.

The ALICE experiment was specifically designed to study heavy-ion physics at the LHC, namely the properties of strongly interacting matter at high energy density. The first LHC heavy-ion run took place at the end of 2010 with Pb–Pb ions accelerated at a centre-of-mass energy  $\sqrt{s_{NN}} = 2.76$  TeV. The ALICE detector collected almost  $30 \times 10^6$  nuclear interaction minimum bias triggers. The analysis described in this paper is mainly based on the sub-detectors mentioned in the following. The tracking and vertexing are performed with the full tracking system: the Inner Tracking System (ITS, six layers of silicon detectors) and the Time Projection Chamber (TPC), which is also used for particle identification via specific ionization. The Silicon Pixel Detector (SPD, the two innermost layers of the ITS) and the VZERO detector (scintillation hodoscopes placed on either side of the interaction point) were used for triggering. The VZERO was crucial for the centrality definition as well. A complete description of the ALICE sub-detectors can be found in [4], whereas the trigger selection strategy and the procedure to determine centrality are described in [5].

## 2. Reconstruction of multi-strange baryons

Multi-strange baryons are measured through the reconstruction of the topology of the following weak decays:  $\Xi^- \rightarrow \pi^- + \Lambda$ ,  $\Omega^- \rightarrow K^- + \Lambda$  (with  $\Lambda \rightarrow \pi^- + p$ ) plus the charge conjugates for the anti-particle decays. The resulting branching ratios are 63.9% and 43.3% for the  $\Xi$  and the  $\Omega$ , respectively. The  $\Xi$  and the  $\Omega$  candidates are found by combining reconstructed charged tracks: cuts on geometry and kinematics, *e.g.* related to the impact parameter of the tracks and the invariant masses, are applied to select first, the  $\Lambda$  candidate and then, to match it with all the remaining secondary tracks (bachelor candidates). Only candidates satisfying tighter selections contribute to the analysis. In particular, cuts on particle identification via specific ionization in the TPC for the three daughter tracks are imposed. Examples of the invariant mass distributions before and after the tightening of the cuts are shown in Fig. 1: the set of tighter cuts allows the background to be significantly reduced without losing a considerable fraction of the signal.

To extract the signal in  $p_T$  intervals, a symmetric region around the peak ( $\pm 3\sigma$ ) is defined fitting the distribution with the sum of a Gaussian and a polynomial. The background is sampled on both sides of the peak in two regions  $6\sigma$  wide and  $6\sigma$  away from the peak and fitted with a polynomial of

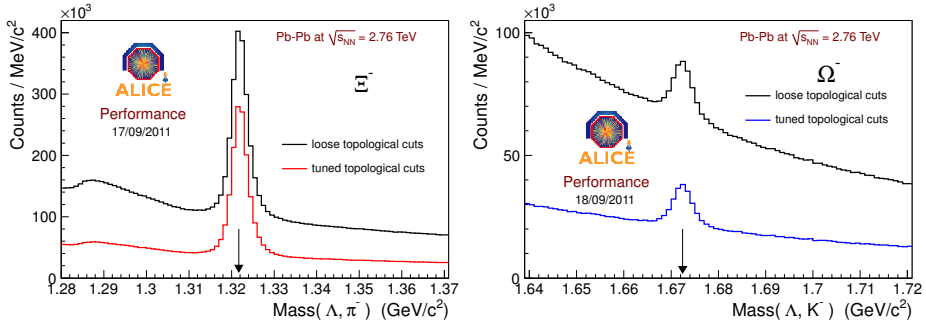


Fig. 1. Invariant mass distributions for the  $\Xi^-$  (left panel) and the  $\Omega^-$  candidates (right panel) integrated over  $p_T$  and centrality with two different sets of cuts: loose cuts for candidate reconstruction (black histograms) and final cuts for the analysis (grey/coloured histograms). TPC PID is requested for the three daughters in both cases.

second degree (first degree for high  $p_T$  bins). In each  $p_T$  bin the signal in the peak region is obtained subtracting the integral of the fit function of the background from the peak population.

### 3. Efficiency and acceptance correction

To correct the data as a function of  $p_T$ , about  $3 \times 10^6$  events were generated using HIJING [6]: events were enriched with one cascade of each species, multi-strange baryons being rarely produced. It has been verified that the efficiency is not biased by the presence of injected signals. In Fig. 2 examples of the efficiency factors for two centrality classes are shown: as expected, the efficiency increases going from the most central to the most peripheral events.

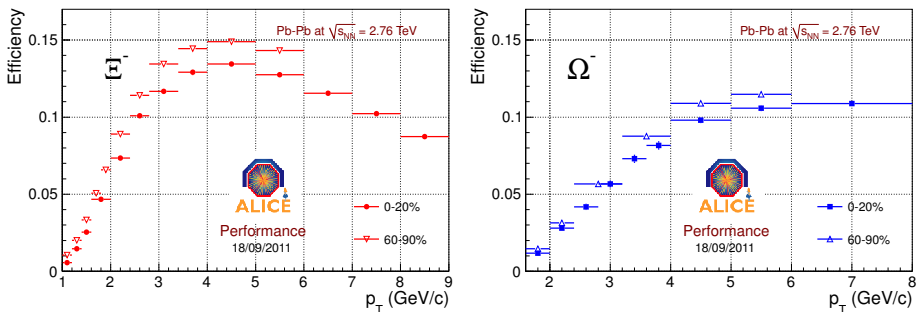


Fig. 2. Efficiency factors (including acceptance and branching ratios) as a function of  $p_T$  in the rapidity window  $|y| < 0.5$  for the  $\Xi^-$  (left panel) and for the  $\Omega^-$  (right panel) in two centrality classes (most central and most peripheral).

## 4. Results

The analysis has been performed on a sample of about  $20 \times 10^6$  events, by both integrating in centrality (0–90%) and dividing it in four classes (0–20%, 20–40%, 40–60%, 60–90%). In the left panel of Fig. 3 the corrected spectra in 0–90% centrality are shown with the error bars representing the sum in quadrature of the statistical and systematic uncertainties. In the right panel of Fig. 3 the ratios of anti-particle over particle spectra are shown: they are compatible with unity within the uncertainties, confirming the expectation at the LHC energies.

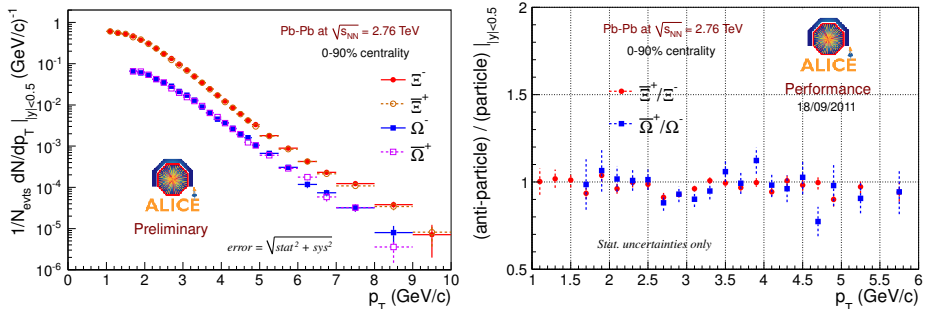


Fig. 3. Left panel: corrected  $p_T$  spectra of the  $\Xi$  and the  $\Omega$  in 0–90% centrality. Right panel: ratio of spectra of anti-particles over particles.

In Fig. 4 the corrected spectra are shown in centrality classes for the  $\Xi^-$  and the  $\Omega^-$ . Similar spectra have been obtained for the anti-particles.

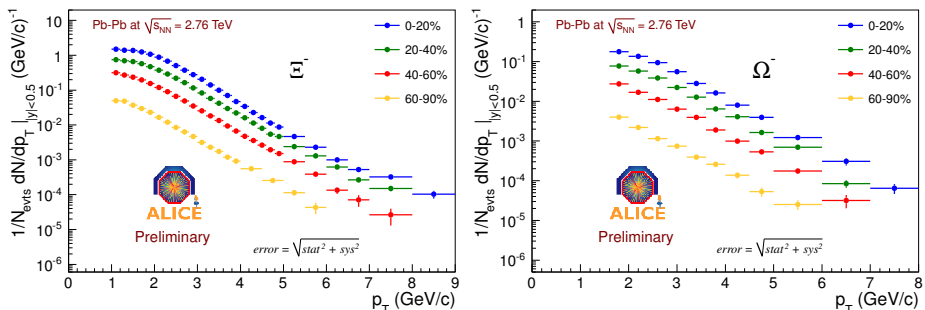


Fig. 4. Corrected  $p_T$  spectra of the  $\Xi^-$  (left panel) and the  $\Omega^-$  (right panel) in four centrality classes.

In order to extract particle yields integrated over the full  $p_T$  range, the spectra are fitted using the blast-wave parametrization [7]. Yields then are calculated integrating the corrected spectra in the measured  $p_T$  range and extrapolating with the fit function outside.

Several contributions to the systematic uncertainty of particle spectra have been studied, in particular those coming from signal extraction, topological and kinematical selection cuts, centrality range for the efficiency calculation. The dominant contribution comes from the centrality dependence of the efficiency correction and makes up almost the total systematic uncertainty which is about 10% in all  $p_T$  bins. To evaluate the systematic uncertainty on the extrapolation at low  $p_T$  for yield extraction, several fit functions have been compared to the blast-wave shape, such as exponential in transverse mass, Boltzmann and Lévy functions [8]. The additional contribution to the systematic uncertainty on the yields is 10% for the  $\Xi$  and 15% for the  $\Omega$ .

The enhancements have been calculated as the ratio between the yields in Pb–Pb collisions and those in  $pp$  interactions at the same energy, both normalized to the number of participants. The  $pp$  reference values were obtained interpolating ALICE data at two energies ( $\sqrt{s} = 0.9$  and 7 TeV [9, 10]) for the  $\Xi$  and STAR data at 200 GeV and ALICE data at 7 TeV for the  $\Omega$ . For both particles, the excitation function of PYTHIA yields (Perugia 2011 tune 88 S350 [11]) is assumed: despite a constant underestimation of the yields [10], its energy dependence in  $s^{0.13}$  (which is slightly higher than the one for charged-particle pseudorapidity density, *i.e.*  $s^{0.11}$  [12]) is consistent with measurements. In Fig. 5 the enhancements as a function of the mean number of participants are shown (full symbols): they increase with centrality and with the strangeness content of the particle as already observed at lower energies.

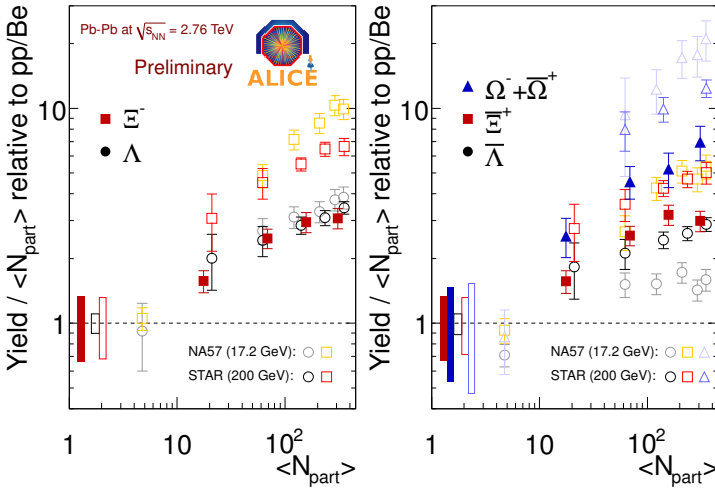


Fig. 5. Enhancements in  $|y| < 0.5$  as a function of the mean number of participants  $N_{\text{part}}$  measured by ALICE and compared to SPS and RHIC data. The bars on the dotted line indicate the systematic uncertainties on the  $pp$  reference.

Comparing the ALICE measurements with those at SPS and RHIC (hollow symbols), the enhancements are found to decrease as the centre-of-mass energy increases, continuing the same trend established at lower energies and first observed at SPS [2].

## 5. Conclusions

ALICE has measured multi-strange baryon spectra in Pb–Pb interactions at  $\sqrt{s_{NN}} = 2.76$  TeV up to  $p_T = 9$  GeV/ $c$  for the most central events. The enhancements have been also measured in four centrality classes: they increase with centrality following the hierarchy based on the strangeness content of the particle. The comparison with lower energy data results shows that the enhancements decrease with increasing energy as already observed at SPS and between SPS and RHIC.

## REFERENCES

- [1] J. Rafelski, B. Müller, *Phys. Rev. Lett.* **48**, 1066 (1982); P. Koch, J. Rafelski, W. Greiner, *Phys. Lett.* **B123**, 151 (1983); P. Koch, B. Müller, J. Rafelski, *Phys. Rep.* **142**, 167 (1986).
- [2] B.I. Abelev *et al.* [STAR Collaboration], *Phys. Rev.* **C77**, 044908 (2008); F. Antinori *et al.* [NA57 Collaboration], *J. Phys. G* **32**, 427 (2006); F. Antinori *et al.* [NA57 Collaboration], *J. Phys. G* **37**, 045105 (2010).
- [3] J. Schaffner-Bielich, *J. Phys. G* **30**, R245 (2004).
- [4] K. Aamodt *et al.* [ALICE Collaboration], *JINST* **3**, S08002 (2008).
- [5] K. Aamodt *et al.* [ALICE Collaboration], *Phys. Rev. Lett.* **106**, 032301 (2011).
- [6] X.-N. Wang, M. Gyulassy, *Phys. Rev.* **D44**, 3501 (1991).
- [7] E. Schnedermann, J. Sollfrank, U. Heinz, *Phys. Rev.* **C48**, 2462 (1993).
- [8] C. Tsallis, *J. Stat. Phys.* **52**, 479 (1988).
- [9] K. Aamodt *et al.* [ALICE Collaboration], *Eur. Phys. J.* **C71**, 1594 (2011).
- [10] A. Maire [ALICE Collaboration], *Acta Phys. Pol. B Proc. Suppl.* **5**, 231 (2012), this issue.
- [11] P.Z. Skands, *Phys. Rev.* **D82**, 074018 (2010).
- [12] K. Aamodt *et al.* [ALICE Collaboration], *Phys. Rev. Lett.* **105**, 252301 (2010).